Fuzzy Color Extractor Based Algorithm for Segmenting an Odor Source in Near Shore Ocean Conditions

Wei Li, Yunyi Li, and Jianwei Zhang

Abstract—**A mission of chemical plume tracing (CPT) in near-shore and ocean environments is to find out an odor source via an autonomous underwater vehicle (AUV). It is necessary to confirm the detected odor source using a visual system interactively or automatically, when a chemical sensor identifies the odor source. However, color images taken in near-shore ocean environments are very vague due to dim illumination conditions and fluid advection effects.**

This paper presents a fuzzy algorithm for recognizing the chemical plume and its source in near-shore and ocean environments. This algorithm iteratively generates color patterns based on a defined reference color and extracts color components of the chemical plume and its source from fuzzy images using a fuzzy color extractor (FCE). The proposed approach to color image segmentation might be of general interest to robot vision.

I. Introduction

In order to develop an autonomous underwater vehicle (AUV) based chemical plume tracer for natural fluid environment applications, several biologically inspired chemical plume tracing (CPT) strategies were proposed under the CPT program sponsored by ONR/DAPAR [1]-[7]. The moth-inspired ***passive*** and ***active*** plume tracing strategies [7] were implemented on a REMUS underwater vehicle, which has been developed by the Oceanographic Systems Laboratory at the Woods Hole Oceanographic Institute, for in-water test runs. The REMUS is equipped with a variety of sensors, including a fluorometer, side-scan sonar, and conductivity, temperature, and depth sensors. The REMUS also carries sensors to provide information about the current operating state of the vehicle, including the vehicle latitude and longitude, depth and altitude, heading and speed, and water flow velocity. The REMUS vehicle is designed to be small, lightweight, and highly accurate in terms of navigational performance and sensor data. The maximum operation depth is 100 m, and the velocity range is from 0.25 m to 2.8 m/s. The REMUS vehicle contained two PC-104 computers. The first computer system (REMUS) implemented the standard REMUS propulsion, control, navigation, sensor processing algorithms, as well as a pre-programmed CPT strategy. The second computer system implemented the CPT architecture [8], which subsumes four fundamental behavior types: finding a plume, tracing the plume, reacquiring the plume, and declaring the source location. This architecture is the first to take CPT tests from the lab to a complex real environment, and the successful in-water test runs conducted at San Clemente Island, California [8], and in Duck, North Carolina [9], demonstrated chemical plume tracing over 100 m with source declaration accuracy on the order of tens of meters. In order to confirm the identified odor source using a visual system interactively and automatically, a Source-Verification module in the subsumption architecture was proposed for segmenting the chemical plume and its source [10]. However, processing images taken in near-shore, ocean conditions is a very challenging task, since the propagation of light underwater is complicated by three phenomena which affect both the illuminant and the light rays reflected from the object to the sensor: scattering, refraction, and absorption [11]. These facts cause interpretation of color images of real scenes taken in near shore ocean environments usually incomplete and ambiguous [12], and consequently it is very hard to reliably determine which color belongs to and which does not belong to the chemical plume and its source.

This paper proposes an algorithm for segmenting the color components of the chemical plume and its source, based on a fuzzy color extractor (**`FCE`**). The **`FCE`** is directly extended from the fuzzy gray-level extractor, which was applied to recognize landmarks on roads for autonomous vehicle navigation in [13]-[15], i.e., the fuzzy rules for extracting an object from gray-level images

If *the gray level of a pixel is close to the gray level of the road*
Then *make it to black*
Else *make it to white*

are modified to the rules for extracting an object from color images

If *the color components of a pixel closely match the color components of an object*
Then *extract this pixel for the object*
Else *do not extract it*

Colors in the images taken in the near shore ocean environments are not well-defined. In order to segment the chemical plume and its source, the algorithm proposed in this paper defines reference colors to generate color patterns and utilizes the **`FCE`** to extract color components of the chemical plume and its source iteratively. The study results demonstrate that the proposed algorithm is effective to

Manuscript received December 18, 2007. This work was supported in part by the U.S. Office of Naval Research Grant ONR N00014-01-1-0906 under the ONR Chemical Sensing in the Marine Environment Program, the RCU grant at CSUB, and BMBF IVUS project.

W. Li and Y. Y. Li are with the Department of Computer Science, California State University, Bakersfield, CA 93311 USA (wli@cs.csubak.edu).

J. W. Zhang is with Institute TAMS (Technical Aspects of Multimodal Systems), Department of Informatics, University of Hamburg Vogt-Koelln-Strasse 30, D-22527 Hamburg, Germany (zhang@informatik.uni-hamburg.de).

978-1-4244-1819-0/08/$25.00©2008 IEEE

process the fuzzy images taken in the near shore ocean environments.

II. Fuzzy Color Extractor

The partitioning of an image into some sub-images that represent different objects is called segmentation. In many color-based vision applications, however, colors in an image are ambiguous due to environment uncertainty. This paper proposes the fuzzy color extractor to deal with such uncertainty. In this study, colors of an image are described in the RGB space, where colors are represented by their red, green, and blue components in an orthogonal Cartesian space. The color of each pixel $\boldsymbol{p}(m, n)$ denoted by $\boldsymbol{p}(m, n)_{RGB}$ is processed to separate its red, green, and blue components ($\boldsymbol{p}(m, n)_R$, $\boldsymbol{p}(m, n)_G$, $\boldsymbol{p}(m, n)_B$). The **FCE** extracts a cluster of colors based on a defined color pattern (CP or CP_{RGB}). The CP_{RGB} is either directly defined by its RGB components (CP_R, CP_G, CP_B) or determined by a pixel in the image. The color component differences between $\boldsymbol{p}(m, n)_{RGB}$ and CP_{RGB} are calculated as follows:

$$\begin{cases} \boldsymbol{dif}(m,n)_R = \boldsymbol{p}(m,n)_R - CP_R \\ \boldsymbol{dif}(m,n)_G = \boldsymbol{p}(m,n)_G - CP_G \\ \boldsymbol{dif}(m,n)_B = \boldsymbol{p}(m,m)_B - CP_B \end{cases}, \quad 0 \le m < M, \quad 0 \le n < N \tag{1}$$

where M and N indicate the size of an array which holds the image. The following fuzzy rules are applied to $\boldsymbol{dif}(m, n)_R$, $\boldsymbol{dif}(m, n)_G$, and $\boldsymbol{dif}(m, n)_B$:

If $\boldsymbol{dif}(m, n)_R$ *and* $\boldsymbol{dif}(m, n)_G$ *and* $\boldsymbol{Dif}(m, n)_B$ *are* **Zero**
Then $\boldsymbol{p}(m, n)$ *is* **Matched**
If $\boldsymbol{dif}(m, n)_R$ *or* $\boldsymbol{dif}(m, n)_G$ *or* $\boldsymbol{Dif}(m, n)_B$ *is* **Negative** *or* **Positive**
Then $\boldsymbol{p}(m, n)$ *is* **Unmatched**

Both the rules indicate that the pixel, $\boldsymbol{p}(m, n)$, belongs to the object to be extracted, if the Euclidean distances between $\boldsymbol{p}(m, n)_{RGB}$ and CP_{RGB} along the three axes in RGB coordinate system are small enough; otherwise, $\boldsymbol{p}(m, n)$ does not belong to the object. Fig. 1(a) shows the membership functions ($\mu_N(x)$, $\mu_Z(x)$, $\mu_P(x)$) for the input fuzzy variables (**Negative**, **Zero**, **Positive**) defined by

$$\mu_{\mathbf{N}}(x) = \begin{cases} 1 & -255 \le x < -\alpha_2 \\ \dfrac{(x + \alpha_1)}{(\alpha_1 - \alpha_2)} & -\alpha_2 \le x < -\alpha_1 \\ 0 & -\alpha_1 \le x \le 255 \end{cases}, \tag{2}$$

$$\mu_{\mathbf{Z}}(x) = \begin{cases} 0 & -255 \le x < -\alpha_2 \\ \dfrac{(x + \alpha_2)}{(\alpha_2 - \alpha_1)} & -\alpha_2 \le x < -\alpha_1 \\ 1 & -\alpha_1 \le x < \alpha_1 \\ \dfrac{(x - \alpha_1)}{(\alpha_2 - \alpha_1)} & \alpha_1 \le x < \alpha_2 \\ 0 & \alpha_2 \le x \le 255 \end{cases}, \tag{3}$$

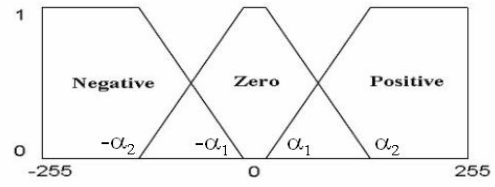

(a) Membership functions for color differences.

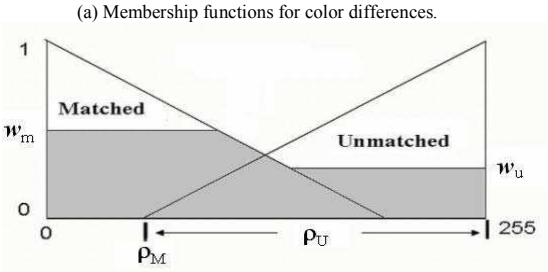

(b) Membership functions for defuzzification

Fig. 1: Membership functions for color image segmentation.

$$\mu_{\mathbf{P}}(x) = \begin{cases} 0 & -255 \le x < \alpha_1 \\ \dfrac{(x - \alpha_1)}{(\alpha_2 - \alpha_1)} & \alpha_1 \le x < \alpha_2 \\ 1 & \alpha_2 \le x \le 255 \end{cases}, \tag{4}$$

and Fig. 1(b) shows the membership functions ($\mu_M(x)$, $\mu_U(x)$) for the output fuzzy variables (**Matched**, **Unmatched**) defined by

$$\mu_{\mathbf{M}}(x) = \begin{cases} \dfrac{(\rho_M - x)}{\rho_M} & 0 \le x \le \rho_M \\ 0 & \rho_M \le x \le 255 \end{cases}, \tag{5}$$

$$\mu_{\mathbf{U}}(x) = \begin{cases} 0 & 0 \le x \le \rho_U \\ \dfrac{(x - \rho_U)}{(255 - \rho_U)} & \rho_U \le x \le 255 \end{cases}, \tag{6}$$

where $\rho_M + \rho_U = 255$. Based on $\boldsymbol{dif}(m, n)_R$, $\boldsymbol{dif}(m, n)_G$, and $\boldsymbol{dif}(m, n)_B$, the fuzzy rules produce the weight w_m for **Matched** and the weight w_u for **Unmatched** by

$$\begin{aligned} w_m &= \mathbf{min}\{w_{m(R)}, w_{m(G)}, w_{m(B)}\} \\ w_u &= \mathbf{max}\{w_{u(R)}, w_{u(G)}, w_{u(B)}\} \end{aligned}. \tag{7}$$

Fig. 1(b) shows the produced areas in the output domain while w_m and w_u cutting $\mu_M(x)$ and $\mu_U(x)$. A crisp output value, $\Delta\rho_F$, is calculated by the centroid defuzzification method

$$\Delta\rho_F = \frac{\int \mu_{\mathbf{out}}(x) x dx}{\int \mu_{\mathbf{out}}(x) dx}, \tag{8}$$

where $\mu_{\mathbf{out}}(x)$ represents the envelope function of the areas cut by w_m and w_u in fuzzy output domain. If $\Delta\rho_F < \varepsilon$, $\boldsymbol{p}(m, n)$ is extracted; otherwise, $\boldsymbol{p}(m, n)$ is not extracted, where ε is a threshold. The **FCE** can be understood as a mapping operator between Euclidean distances $\{\boldsymbol{dif}(m, n)_R, \boldsymbol{dif}(m, n)_G, \boldsymbol{dif}(m, n)_B\}$ in the RGB space and a difference $\Delta\rho_F$ in the intensity space under a fuzzy metric. We propose the procedure **FuzzyColorSeg** to segment some objects from a color

image.

FuzzyColorSeg(I_S)
  $CP_{RGB} \leftarrow$ **GetCP**(I_S);
  $[I_U, I_M] \leftarrow$ **FCE**(I_S, CP_{RGB});
  return $[I_U, I_M]$;

FuzzyColorSeg invokes two procedures: **GetCP** and **FCE**. **GetCP** generates a CP_{RGB} for **FCE** to split a source image I_S into two sub-images: one sub-image, I_M, holds the matched colors; and the other sub-image, I_U, remains the unmatched colors.

We take the images in Fig. 2 as examples to demonstrate how to extract the flower from the original image $I_U^{(0)}$ –"flower" by **FuzzyColorSeg**. Here, $I_U^{(0)}$ is initialized as the source image I_S for **FuzzyColorSeg**. First, we define three CPs: (255, 0, 0)–red, (0, 255, 0)–green, and (0, 0, 255)–blue, to extract three words "RED", "GREEN", and "BLUE" from $I_U^{(0)}$ –"flower". Based on the CPs, **FCE** extracts the three words from $I_U^{(0)}$ and stores them into $I_M^{(1)}$, as shown in Fig. 2(b). Meanwhile, **FCE** generates $I_U^{(1)}$ by setting the extracted pixels in $I_U^{(0)}$ to white. $I_U^{(1)}$, expressed by $I_U^{(0)} = I_U^{(1)} \cup I_M^{(1)}$, is not displayed in Fig. 2. Then, we select a pixel from the background in $I_U^{(0)}$ –"flower" and define its color components as a new CP_{RGB} to remove background colors in $I_U^{(0)}$ –"flower". Here, the first pixel $\boldsymbol{p}(0, 0)$ in the sub-image $I_U^{(1)}$ is chosen, which is located on the left-bottom corner. Its color components $\boldsymbol{p}(0, 0)_{RGB}$ are (6, 6, 8), being very close to the black color. At this step, **FCE** takes the image $I_U^{(1)}$ as a new source image and splits $I_U^{(1)}$ into the sub-images $I_M^{(2)}$ and $I_U^{(2)}$ again. $I_M^{(2)}$ holds the colors extracted from $I_U^{(1)}$, as shown in Fig. 2(c); while $I_U^{(2)}$ holds the color components of the flower petal, as shown in Fig. 2(d).

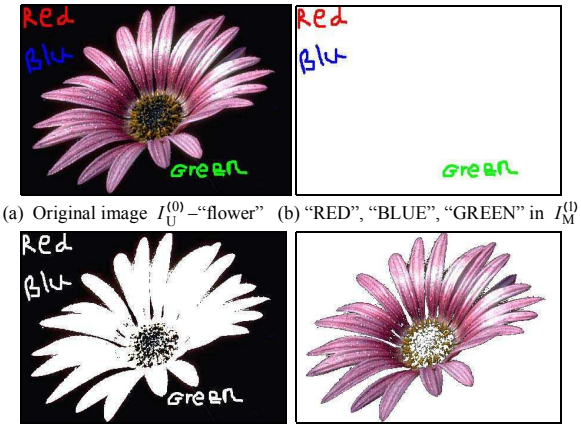

(a) Original image $I_U^{(0)}$ –"flower" (b) "RED", "BLUE", "GREEN" in $I_M^{(1)}$

(c) Background color in $I_M^{(2)}$ (d) Flower colors in $I_U^{(2)}$

Fig. 2: Flower segmentation by fuzzy color extractor

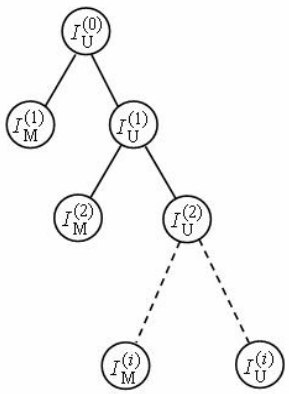

Fig. 3: Iterative procedure for segmentation

III. Iterative Fuzzy Segmentation Procedure

The purpose of this study is to extract the chemical plume and its source from an image taken during the CPT missions. Unfortunately, extracting the chemical plume and its source from such an image is much more difficult than segmenting the flower from the image–"flower" since the color image taken in near-shore oceanic environments is very vague and the objects' colors in the image are significantly distorted from their nature colors due to dim illumination conditions and flow fluid influence. In order to solve this problem, we propose an iterative procedure shown in Fig. 3 to process the image using **FuzzyColorSeg** until the chemical plume and its source are extracted satisfactorily. For convenience, we define two groups of the sub-images $I_M^{(i)}$ and $I_U^{(i)}$ split by **FCE**. $I_M^{(i)}$ contains matched colors after the ith step extraction, while $I_U^{(i)}$ contains unmatched colors. The original image $I_U^{(0)}$ is the initial source image to the procedure, and $I_U^{(i)}$ is the source image for the $(i+1)$th step segmentation. Note that we have the relationship $I_U^{(i)} = I_U^{(i+1)} \cup I_M^{(i+1)}$. In our application, a default color is defined as white with (255, 255, 255) in the RGB space. **FEC** generates $I_M^{(i)}$ by moving the matched pixels from the source image to an image initialized by white color, and generates $I_U^{(i)}$ by setting the extracted pixels in the source image to white color. Obviously, selecting color patterns becomes the key issue of extracting desired objects from an image.

IV. Reference Colors

The difficulty of segmenting the chemical plume and its source from images taken in ocean environments lie in definition of their color patterns, since colors in the vague images are not well defined due to illumination variance and fluid advection affects. We employ some well-defined colors as reference colors to generate CPs. To our

knowledge, the color components of the Rhodamine dye plume are close to the red color, and those of the chemical source are dark and close to the blue color. Therefore, we define the two reference colors: **RED**$_{RGB}$ with (255, 0, 0) and **DARK-BLUE**$_{RGB}$ with (**BLACK**$_{RGB}$+**BLUE**$_{RGB}$)/2 = (0, 0, 128) to generate color patterns for segmenting the chemical plume and the odor source, respectively. We propose the procedure:

```
GetCP(I_s)
    RefColor ← RED_RGB or DARK-BLUE_RGB;
    ||CP_RGB|| ← ∞;
    for m ← 0 to M-1 do
        For n ← 0 to N-1 do
            Dis ← ||RefColor - p(m, n)_RGB||
            if Dis < ||CP_RGB||
                CP_RGB ← p(m, n)_RGB;
    return CP_RGB;
```

where I_s is an image to be processed, M (the maximum row) and N (the maximum column) determine the size of I_s. In order to extract color components of the chemical plume, **RED**$_{RGB}$ is assigned to RefColor, so the procedure returns a CP$_{RGB}$ that holds the color components of the pixel in the image with the shortest Euclidean distance to the reference color – **RED**$_{RGB}$. The following discussion presents how colors of the chemical plume are extracted. $I_U^{(0)}$ is the original image–"odor", as shown in Fig. 4(a), and $I_M^{(1)}$ is initialized as an empty image with white. **FuzzyColorSeg** takes $I_U^{(0)}$ as an input and passes $I_U^{(0)}$ to **GetCP**. **GetCP** defines **RED**$_{RGB}$ as RefColor and returns a CP$_{RGB}$ (106, 106, 231) for $I_U^{(0)}$, listed in Table I. Based on the CP$_{RGB}$, **FCE** splits $I_U^{(0)}$ –"odor" into two sub-images $I_U^{(1)}$ and $I_M^{(1)}$. $I_M^{(1)}$ is produced by moving the extracted pixels from $I_U^{(0)}$ to the empty image and holds color components

TABLE I
CPs BASED ON RED REFERENCE COLOR

Image	CP$_{RGB}$	Distance	Intensity
$I_U^{(0)}$	CP$_{RGB}$ (106, 106, 231)	295	148
$I_U^{(1)}$	CP$_{RGB}$ (156, 136, 243)	296	178
$I_U^{(2)}$	CP$_{RGB}$ (120, 144, 245)	313	170

TABLE II
CPs BASED ON DARK-BLUE COLOR

Image	CP$_{RGB}$	Distance	Intensity
$I_U^{(3)}$	CP$_{RGB}$ (65, 100, 240)	164	135
$I_U^{(4)}$	CP$_{RGB}$ (26, 131, 236)	171	131
$I_U^{(5)}$	CP$_{RGB}$ (66, 136, 241)	189	147
$I_U^{(6)}$	CP$_{RGB}$ (29, 170, 232)	201	145

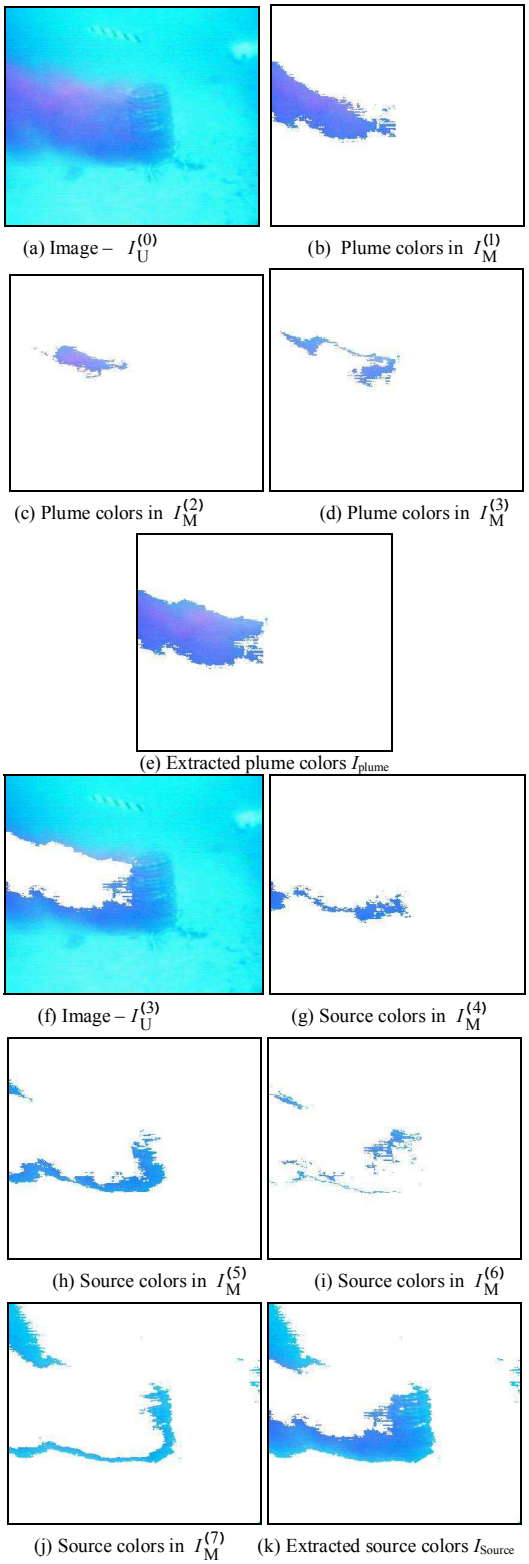

(a) Image – $I_U^{(0)}$ (b) Plume colors in $I_M^{(1)}$
(c) Plume colors in $I_M^{(2)}$ (d) Plume colors in $I_M^{(3)}$
(e) Extracted plume colors I_{plume}
(f) Image – $I_U^{(3)}$ (g) Source colors in $I_M^{(4)}$
(h) Source colors in $I_M^{(5)}$ (i) Source colors in $I_M^{(6)}$
(j) Source colors in $I_M^{(7)}$ (k) Extracted source colors I_{Source}

Fig. 4: Extraction of the chemical plume and source

closely match to the CP_{RGB}. $I_U^{(1)} = I_U^{(0)} - I_M^{(1)}$ is produced by setting the extracted pixels to white in $I_U^{(0)}$. $I_M^{(1)}$ is the first segmented image for the chemical plume, as shown in Fig. 4(b). The chemical plume in the image is not completely extracted since the chemical colors are distorted due to environmental illumination variation and fluid advection affects. The further segmentation needs $I_U^{(1)}$ as a new source image for the next step segmentation. **FuzzyColorSeg** takes $I_U^{(1)}$ as its input, and **GetCP** gets a new CP_{RGB} with (156, 136, 243) listed in Table I for $I_U^{(1)}$. Based on the new CP_{RGB}, **FCE** splits the image $I_U^{(1)}$ into two sub-images $I_U^{(2)}$ and $I_M^{(2)}$. Similarly, $I_M^{(2)}$ is produced by moving the extracted pixels from $I_U^{(1)}$ to an empty image and holds the color components closely matching to the new CP_{RGB}. $I_M^{(2)}$ represents the second segmented image for the chemical plume, as shown in Fig. 4(c). $I_U^{(2)}$ is generated by setting the extracted pixels from $I_U^{(1)}$ to white. At the *i*th step, **FuzzyColorSeg** split $I_U^{(i)}$ into $I_U^{(i+1)}$ and $I_M^{(i+1)}$. Fig. 4(d) displays the segmented image $I_M^{(3)}$ at the third step. The union operation $I_{plume} = I_M^{(1)} \cup I_M^{(2)} \cup I_M^{(3)}$ generates the segmented chemical plume, as shown in Fig. 4(e). The $\mathbf{RED}_{RGB}$–based CPs are listed in Table I.

In order to extract the chemical source, $\mathbf{DARK\text{-}BLUE}_{RGB}$ is assigned to RefColor, and **FuzzyColorSeg** takes $I_U^{(3)}$ as the input that is the image after the chemical plume is extracted, as shown in Fig. 4(f). **GetCP** returns a CP_{RGB} with (65, 100, 240) that holds the colors of the pixel in $I_U^{(3)}$ with the shortest Euclidean distance to $\mathbf{DARK\text{-}BLUE}_{RGB}$, listed in Table 2. Based on this CP_{RGB}, **FCE** split $I_U^{(3)}$ into two sub-images $I_U^{(4)}$ and $I_M^{(4)}$. $I_M^{(4)}$ contains the color components of the chemical source, as shown in Fig. 4(g). This procedure continues four steps to extract the color components of the chemical source, as shown in Fig. 4(g)-(l). The union operation $I_{source} = I_M^{(4)} \cup I_M^{(5)} \cup I_M^{(6)} \cup I_M^{(7)}$ generates the extracted color components of the chemical source shown in Fig. 4(k).

The extracted colors in $I_M^{(i)}$ can be understood as a fuzzy color cluster under the given membership function. For segmenting colors in the images in Fig. 4, we choose the parameters of the membership functions as follows: α_1=35, α_2=200, ρ_M=20, ρ_U=235, and ε=80. In this study, we consider two criteria for clustering the colors extracted by **FCE**: The first is based on the distances of the CPs to their associated reference color, and the second based on the relative distances between the CPs. For the first criterion, we take the CP_{RGB} with the shortest distance to the given reference color as a pivot, e.g., the CP_{RGB} with the distance of 295 in Table I and the one with the distance of 164 in Table II, respectively. Then, we calculate the differences

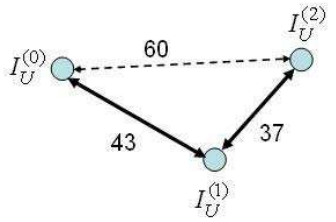

(a) Graph for color patterns for the chemical plume

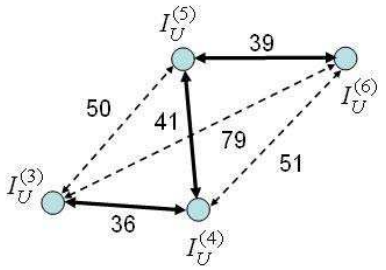

(b) Graph for color patterns for the chemical plume

Fig. 5: Classifying color components of the chemical plume and source based on color patterns

between distances of the pivot and any other CPs in this group: $\Delta_1 = \|CP_{RGB}\| - \|Pivot_{RGB}\|$. If $\Delta_1 > \varepsilon_1$, its corresponding CP_{RGB} is excluded from this group. For the second criterion, we construct a graph based on the distances between the CPs in terms of the given reference color. Then, we start with the pivot in a graph to calculate the shortest distances using Floyd's algorithms. The CP_{RGB} is removed from this graph, if its shortest distance is greater than ε_2. Fig. 5(a)-(b) shows the graphs of the CPs in Tables I and II and their shortest distances. Both the criteria ensure that the CPs in a group are close to their pivot enough. In this paper, we select ε_1 and ε_2 as 40 and 45.

Tables I and II also provide the corresponding intensities of the CPs, which are computed by ρ=(R+G+B)/3. Our experiment results show that human eyes might not sensitively reflect the color changes if the Euclidean distance of two colors in the RGB space is less than 25 and their intensity difference is less than 10. Although we may slightly sense the variations between the extracted colors of the chemical plume in $I_M^{(1)}$, $I_M^{(2)}$, and $I_M^{(3)}$ (or those of the odor source in $I_M^{(4)}$, $I_M^{(5)}$, $I_M^{(6)}$, and $I_M^{(7)}$), we cluster them in the same group. We also note that the blue color components of the CPs have the least significant variations.

V. Discussions and Conclusions

CPT missions in near-shore, oceanic environments are very difficult due to complicated flow fluid features affected by turbulence, tides, and waves. It is necessary to identify the declared odor source by a visual system. However, processing images taken in near-shore and ocean conditions is difficult since the propagation of light underwater is affected by scattering, refraction, and absorption. Forward scatter generally leads to a blur in the images and backward

scatter generally limits the contrast of underwater images by creating a "veiling glow". Absorption of light results in that a large amount of light is lost with increased depth from the air-water surface. Also, refraction, which causes light rays to bend while passing from one medium to another, is the reason for over– or under-estimation of depth. The work in [12] discusses their effects in detail.

This paper presents an initial attempt to segment the required objects from the images taken in near-shore oceanic environments using the **FCE**-based algorithm. The study results demonstrate that the proposed algorithm is simple and effective. In [20], we proposed an alternative strategy for segmenting the chemical plume and its source by removing sea water colors iteratively, starting with the color patterns of background in the image. Note that membership functions, which can be viewed as a fuzzy metric to measure colors, may affect the segmented sub-images, i.e., different membership functions generate different color sets from the same image. Our further research will report **FCE**-based segmentation algorithms in other coding spaces, e.g., the brightness-hue-saturation coding. Using a wider deviation from the reference color might be another way to segment colors using **FCE**. However, choosing such a deviation needs an adaptive procedure as the deviation greatly depends on objects to be extracted and significantly varies from case to case, which is less robust and more time consuming than the iterative procedure.

Image segmentation is a fundamental issue in image processing and computer vision. Especially, color images can provide much more information than gray-level, so algorithms for color image segmentation have attracted more and more attention. A number of image segmentation techniques have been proposed in past decades [16]-[18]. However, most of the proposed techniques provide a crisp segmentation of images, where each pixel is classified into a unique subset. This classification may not reflect an understanding of images by human very well, as [16] stated "the image segmentation problem is basically one of psychophysical perception, and therefore not susceptible to a purely analytical solution". Probably, one of the difficulties in color image segmentation is how to define color conception, since an understanding of colors in an image varies by different observers. Moreover, uncertainty and ambiguity must be dominantly considered in many real applications.

Generally, using vision sensors in underwater applications has certain demands in the future, e.g., for shallow water applications, like monitoring marine life or servicing of marine equipment, vision can be a valuable sensing medium. To develop visually-guided underwater vehicles that make underwater vehicles autonomous, development of effective and robust algorithms suited for color image processing in oceanic environments is an absolute necessity. In order to test performance of image processing, the work in [19] presents a comparison for three key visual tracking algorithms used for servo control in ocean conditions.

ACKNOWLEDGMENT

The author would like to thank the Chemical Sensing in the Marine Environment group for their efforts in making the moth-inspired CPT strategies in-water experiments possible.

REFERENCES

[1] J. H. Belanger and M. A. Willis, "Adaptive control of chemical - guided location: Behavioral flexibility as an antidote to environmental unpredictability," *Adaptive Behavior*, vol. 4, pp. 217-253, 1998.

[2] F. W. Grasso, T. R. Consi, D. C. Mountain, and J. Atema, "Biomimetic robot lobster performs chemo-orientation in turbulence using a pair of spatially separated sensors: Progress and challenges," *Robotics and Autonomous Systems*, vol.30, pp. 115-131, 2000.

[3] F. W. Grasso and J. Atema, "Integration of flow and chemical sensing for guidance of autonomous marine robots in turbulent flows," *Journal of Environmental Fluid Mechanics*, vol. 1, pp. 1-20, 2002.

[4] Q. Liao and E. A. Cowen, "The information content of a scalar plume – A plume tracing perspective," *Environmental Fluid Mechanics*, vol. 2, no. 1-2, pp. 9-34, 2002.

[5] M. J. Weissburg et al., "A multidisciplinary study of spatial and temporal scales containing information in turbulent chemical plume tracking," *Environmental Fluid Mechanics*, vol. 2, no. 1-2, pp. 65-94, 2002.

[6] A. T. Hayes, A. Martinoli, and R. M. Goodman, "Distributed chemical source localization," *IEEE Sensors Journal*, vol. 2, pp. 260-271, 2002.

[7] W. Li, J. A. Farrell, and R. T. Cardé, "Tracking of fluid-advected chemical plumes: Strategies inspired by insect orientation to pheromone," *Adaptive Behavior*, vol.9, pp.143-170, 2001.

[8] W. Li, J. A. Farrell, S. Pang, and R. M Arrieta, "Moth-inspired chemical plume tracing on an autonomous underwater vehicle", *IEEE Transactions on Robotics*, vol.22, no.2, pp.292-307, 2006.

[9] J. A. Farrell, S. Pang, and W. Li, "Chemical plume tracing via an autonomous underwater vehicle," *IEEE Journal of Ocean Engineering*, vol.30, pp.428-442, 2005.

[10] W. Li, M. M. Elgassier, C. Bloomquist, and K. Srivastava, "Mulisensor integration for declaring the odor source of a plume in turbulent fluid-advected environments," *in Proc of the 2006 IEEE/RSJ*, pp.5534-5539, 2006.

[11] T. T. Team, "The physics of diving: Light and vision," http://library.thinkquest.org/28170/35.html.

[12] J. S. Jaffe, et al., "Underwater optical imaging: status and prospects", *Oceanography*, vol. 14, pp. 64-75, 2002.

[13] W. Li, G. T. Lu, and Y. Q. Wang: "Recognizing white line markings for vision-guided vehicle navigation by fuzzy reasoning," *Pattern Recognition Letters,* vol.18, no.8, pp.771-780, 1997.

[14] W. Li, and X. J. Jiang: "Road recognition for navigation of an autonomous vehicle by fuzzy reasoning," *Fuzzy Sets and Systems,* vol.93/3, pp.275-280, 1998.

[15] W. Li, F. M Wahl, J. Z Zhou, H Wang, and K. Z He, "Vision-based behavior control of autonomous systems by fuzzy reasoning," *Modeling and Planning for Sensor-Based Intelligent Robot Systems*, pp.311-325, Springer-Verlag, Germany, 1999.

[16] K. S. Fu and J. K. Mui, "A survey on image segmentation," *Pattern Recognition*, vol. 13, pp. 3-16, 1981.

[17] S. K. Pal et al, "A review on image segmentation techniques," *Pattern Recognition*, vol. 29, pp. 1277-1294, 1993.

[18] H. D. Cheng, X. H. Jiang, Y. Sun, and J. L. Wang, "Color image segmentation: Advances & Prospects," *Pattern Recognition*, vol. 34, pp. 2257-2281, 2001.

[19] J. Sattar and G. Dudek, "On the performance of color tracking algorithms for underwater robots under varying lighting and visibility," in *Proc of IEEE ICRA'06*, pp.3550- 3555, 2006

[20] W. Li, "An iterative fuzzy segmentation algorithm for recognizing an odor source in near shore ocean environments," in *Proc of the 2007 IEEE CIRA'07*, pp.101-106, 2007.